

Firdaus Basrawi

Energy Sustainability Focus Group,
Faculty of Mechanical Engineering,
Universiti Malaysia Pahang,
Pekan Pahang 26600, Malaysia
e-mail: mfirdausb@ump.edu.my

Thamir K. Ibrahim

Energy Sustainability Focus Group,
Faculty of Mechanical Engineering,
Universiti Malaysia Pahang,
Pekan Pahang 26600, Malaysia
e-mails: thamirmathcad@yahoo.com;
thamir@ump.edu.my

Giok Chui Lee

Energy Sustainability Focus Group,
Faculty of Mechanical Engineering,
Universiti Malaysia Pahang,
Pekan Pahang 26600, Malaysia
e-mail: gcllee@ump.edu.my

Khairul Habib

Department of Mechanical Engineering,
Universiti Teknologi Petronas,
Bandar Seri Iskandar,
Tronoh 31750, Perak, Malaysia
e-mail: khairul.habib@petronas.com.my

Hassan Ibrahim

Energy Sustainability Focus Group,
Faculty of Mechanical Engineering,
Universiti Malaysia Pahang,
Pekan Pahang 26600, Malaysia
e-mail: drhassan@ump.edu.my

Effect of Solar Fraction on the Economic and Environmental Performance of Solar Air-Conditioning by Adsorption Chiller in a Tropical Region

Solar air-conditioning (AC) is an attractive AC system but it has intermittent output, and therefore, a conventional heater is needed as a backup. This study presents the effect of ratio of heat delivered by solar (Q_{solar}) to the total heat delivered to an adsorption chiller ($Q_{solar} + Q_{heater}$) or solar fraction (SF) on the economic and environmental performance of a solar AC. This solar AC is not a solar-assisted AC, and therefore, it needs to fully cover the cooling load. The cooling demand of an office building in Kuala Lumpur, and the performance of flat-plate collectors and the adsorption chiller were calculated by EQUEST and WATSON software and by a mathematical model, respectively. Economic performance was analyzed by life-cycle cost analysis, whereas the environmental performance was analyzed by using typical emissions rate of energy systems used. It was found that a boiler was a better solution than an electric heater as a backup heater. Furthermore, the net profit (NP) at lower SF was higher because of its lower capital investment, but more emissions were released compared to the conventional AC because of the boiler operation. Thus, when economic and environmental performance were fairly considered, it is appropriate to have solar AC with an SF around 0.74. [DOI: 10.1115/1.4031707]

Keywords: solar air-conditioning, adsorption chiller, solar fraction, economic, emissions

1 Introduction

The number of ACs in Malaysia had increased rapidly from approximately 13,200 units in 1970 to approximately 253,400 in 1997 [1]. This rapid growth has made the government to introduce a new regulation in which only the ACs with energy efficiency ratio of more than 10 are allowed to enter the Malaysian market since 2002 [2]. This demonstrates that only ACs that have good efficiency are available in the Malaysian market. However, it was estimated that the use of AC will reach 1.5×10^6 units by 2020 [1], and this encompasses the need of a better AC method to reduce the power demand for AC in Malaysia.

Solar AC system is an attractive way for AC because it is environmentally friendly and can also reduce the operational cost. Absorption chiller and adsorption chiller are two main pathways for the solar AC. The former is more common because it has higher coefficient of performance (COP) and slightly lower price, but it requires higher regeneration temperature. The latter is comparatively less used because it has lower COP and slightly higher price, but it can operate at lower temperature. This study focuses on the adsorption chiller because it has lower regeneration temperature that lower price flat-plate collectors can provide.

The normal temperature range in which an adsorption chiller can operate is between 60 and 99 °C, and this can be supplied by hot water from flat-plate collectors. In many cases, solar AC is only considered as a solar-assisted AC when the vapor compression AC operates in parallel. In this study, cooling load will be covered fully by an adsorption chiller that was assisted by a backup heater.

Although the tropical region receives solar radiation throughout the year, the insolation fluctuates due to day/night and sunny/cloudy cycle. Therefore, an auxiliary heater that consumes fossil fuel or electricity needs to be operated. The understanding of the ratio of annual average heat delivered by solar (Q_{solar}) to the total annual average heat delivered to an adsorption chiller ($Q_{solar} + Q_{heater}$) or SF is important. The SF will affect the performance of a solar AC because it will determine its size. To obtain more energy from solar and reduce the use of an auxiliary heater, larger flat-plate collector is needed, but this will increase the capital investment of the system. However, if the collector is too small, more fossil fuel/electricity needs to be consumed and this will increase the operational cost and definitely will create more emissions compared to a conventional AC. An optimal size of the collector has to be struck.

Many studies have been done on the design [3–5] and on the performance analysis [6–8] of the adsorption chiller. However, only a few studies have been carried out on the economic performance of the adsorption chiller. Bruno et al. [9] proposed that when a flat-plate collector is used, the adsorption chiller is more

Contributed by the Solar Energy Division of ASME for publication in the JOURNAL OF SOLAR ENERGY ENGINEERING: INCLUDING WIND ENERGY AND BUILDING ENERGY CONSERVATION. Manuscript received May 22, 2015; final manuscript received September 2, 2015; published online October 15, 2015. Assoc. Editor: Jorge E. Gonzalez.

suitable than the absorption chiller. It was also reported that the system cost of the adsorption chiller-based solar AC is higher than H₂O/LiBr absorption chiller-based solar AC [10,11]. Tsoutsos et al. [12] clarified that the adsorption chiller is marginally competitive with a conventional chiller in Greece. Lambert and Beyene [13] concluded that an adsorption chiller is appropriate with a location that has less subsidized electricity rate. Similar conclusion was reported by Fafous et al. which shows that the estimated payback period of a solar AC exceeds the lifetime of the project (24 yr) unless the government issues a new policy that grants incentives, exemptions, and subsidies [14]. Similar result was shown by Allouhi et al. in which an adsorption chiller-based solar AC system had a payback period of 19–23 yr [15]. Environmental performance of the solar AC has been also studied by many researchers, but from the authors' best knowledge, only solar-assisted AC with absorption, instead of adsorption chiller, was studied. Mammoli et al. [16] clarified that a solar-assisted AC can reduce 148–303 kg/day of CO₂ emissions in New Mexico climate. In addition, it was also reported that solar collector area cannot be too small and must exceed certain area to reduce CO₂ emissions [17].

However, from the literature reviewed, there is no report considering the effect of SF on the economic and environmental performance of a solar AC by an adsorption chiller. Thus, the objective of this study is to investigate the effect of SF on the economic and environmental performance of a solar AC by adsorption route. The solar AC studied is not a solar-assisted AC, but the adsorption chiller alone fully covered the cooling load. The cooling load of an office building in Kuala Lumpur was simulated using EQUEST. The amount of heating and its temperature were then determined by using the load required and by the performance of the adsorption chiller. Then, the heating load is covered with flat-plate collectors with various area or SF. Finally, the performance of each SF was calculated and compared using life-cycle cost analysis and emissions reduction.

2 Materials and Methods

2.1 Location and Climatic Data. Weather data of Kuala Lumpur with coordinate of 3.1357° N, 101.6880° E were selected, and hourly weather data from ASHRAE International Weather for Energy Calculation were used. Figure 1 shows the ambient temperature and global horizontal radiation, direct normal radiation, diffuse horizontal radiation, relative humidity, and total sky cover. It can be observed that the hourly average solar radiation is 450–1000 W/m² and the hourly average ambient temperature is around 24–35 °C. The solar radiation varies slightly throughout the year, lower in May, and then increased toward peak in August, decreasing again toward November, and increasing again toward February. Relative humidity is in the range of 36–100%, and the total sky cover is in the range of 1–10 with an average of 8.

2.2 Building Cooling Load. A two-story building was used as a model building. The cooling load of the building was simulated using EQUEST, well-known software for energy building analysis. The office building is shown in Fig. 2 and the parameters used for calculation are shown in Table 1. There was no insulation material considered for the wall and ceiling considering this is the actual practice in Malaysia. As shown in Table 1, the designed ventilation of the building was 0.159 cfm/sf. This building operated from 08:00 to 17:00, Monday to Monday. It was assumed that average number of people in the room was 11 persons, and the number remained constant throughout the operation.

2.3 Adsorption Chiller. The adsorption chiller used was a double bed silica gel–water with maximum cooling capacity of 16 kW. Basic parameters used are shown in Table 2. The

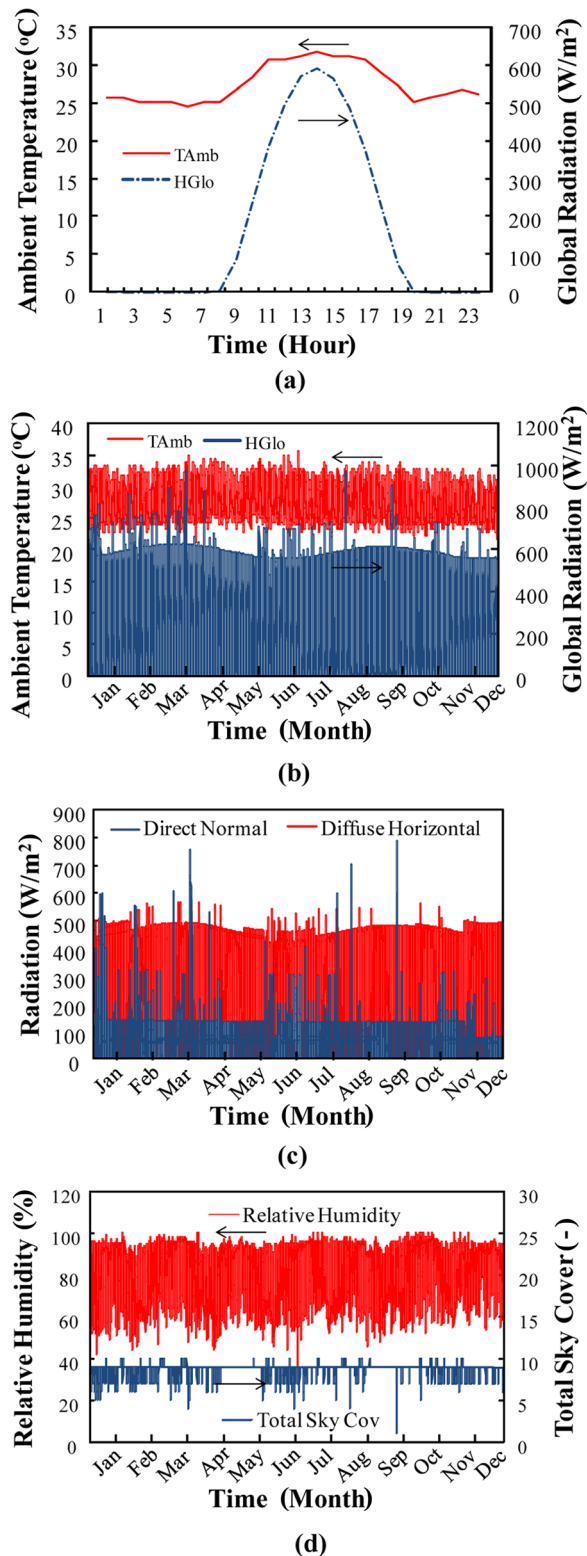


Fig. 1 Weather data of Kuala Lumpur: (a) weather throughout a day, (b) ambient temperature and global horizontal, (c) direct normal and diffuse horizontal, and (d) relative humidity and total sky cover

adsorption rate of the silica gel–water can be expressed from a linear driving force kinetic equation as follows:

$$\frac{dx}{d\tau} = 15 \frac{D_{s0} \exp\left(-\frac{E_a}{RT}\right)}{R_p^2} (x^* - x) \quad (1)$$

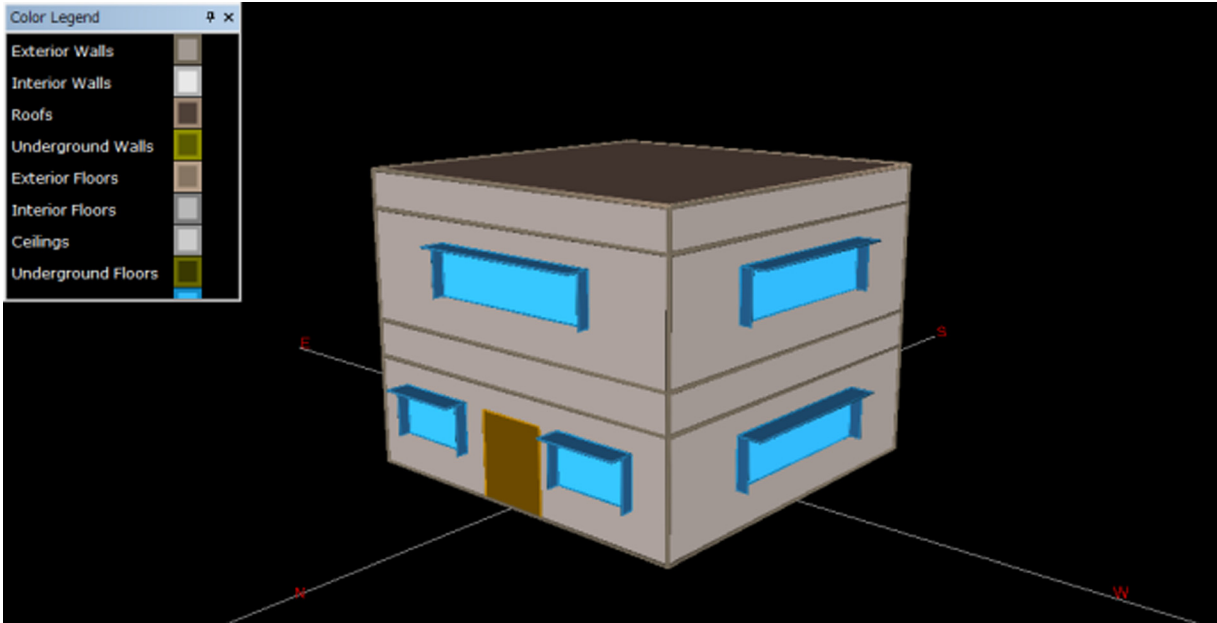


Fig. 2 Overall image of the simulated office building

For silica gel–water system, the modified Freundlich model which is expressed by Eq. (2) is used to estimate the equilibrium uptake, as follows:

$$x^* = \alpha(T_a) \left[\frac{P_s(T_{ref})}{P_s(T_a)} \right]^{\beta(T_a)} \quad (2)$$

where

$$\begin{aligned} \alpha(T_a) &= \alpha_0 + \alpha_1(T_a) + \alpha_2(T_a)^2 + \alpha_3(T_a)^3 \\ \beta(T_a) &= \beta_0 + \beta_1(T_a) + \beta_2(T_a)^2 + \beta_3(T_a)^3 \end{aligned} \quad (3)$$

Table 1 Parameters of the simulated office building

Building shape		Rectangle
Building orientation		North
Running hours	hr	9 (8:00–17:00)
Wall layer		Plaster–clay brick–plaster
Width	m	9.14
Building area	m ²	183.5
Wall height	m	2.7
Ceiling to second floor height	m	0.91
Indoor setting temperature	°C	24
Design ventilation	cfm/sf	0.159
Average number of occupants	people	11

Table 2 Parameters of the adsorption chiller

Mass of the adsorbent, m_a	kg	40
Heat transfer coefficient and area of the bed, UA_{bed}	kW/K	3.50
Heat transfer coefficient and area of the evaporator, UA_{eva}	kW/K	4.87
Heat transfer coefficient and area of the condenser, UA_{con}	kW/K	15.33
Mass of the condenser, m_{con}	kg	24.28
Mass of the evaporator, m_{eva}	kg	12.45
Specific heat of the adsorbent, $C_{p,a}$	kJ/kg K	0.96
Latent heat of working fluid, h_{fg}	kJ/kg	2800
Specific heat of the heat exchanger, $C_{p,hex}$	kJ/kg K	0.95

Using the lumped approach, the energy balance for the sorption bed of silica gel–water pair can be calculated by the following equation:

$$\begin{aligned} [m_a(C_{p,a} + C_{p,ref}x) + m_{hex}C_{p,hex}] \frac{dT_{bed,ref}}{d\tau} \\ = m_a \Delta h_{st} \frac{dx_{bed,ref}}{d\tau} + \gamma m_a C_{p,v,ref} \frac{dx_{bed,ref}}{d\tau} + \dot{m}_f C_{p,f} (T_{bed,in} - T_{bed,out}) \end{aligned} \quad (4)$$

where $\gamma = 1$ for reactor working as adsorber and $\gamma = 0$ for reactor working as desorber. The left-hand side of adsorber/desorber energy balance in Eq. (4) indicates the rate of change of internal energy due to the thermal mass of adsorbent(s), the refrigerant, and adsorber/desorber heat exchanger during adsorption and desorption. The first term on the right-hand side represents the adsorption or desorption heat, and the second term represents for energy transport due to refrigerant vapor transfer from evaporator to adsorbent bed during adsorption–evaporation process. The third term defines the total amount of heat released to the cooling water upon adsorption or provided by the heating source (hot water) for desorption. For a small temperature difference across heating/cooling fluid such as water, the outlet temperature of the source is sufficiently accurate to be modeled by the log mean temperature difference (LMTD) method and it is given by the following equation:

$$\frac{T_{bed,out} - T_{bed}}{T_{bed,in} - T_{bed}} = \exp \left[- \frac{(UA)_{bed,ref}}{\dot{m}_f C_{p,f}} \right] \quad (5)$$

The energy balance equation and outlet temperature for the evaporator and condenser can be expressed by the following equations, respectively:

$$\begin{aligned} (m_{eva} C_{p,eva} + m_{eva,hex} C_{p,hex}) \frac{dT_{eva,ref}}{d\tau} \\ = -h_{fg} m_a \frac{dx_{ads}}{d\tau} + m_a C_{p,ref} (T_{eva} - T_{con}) \\ + \dot{m}_f C_{p,f} (T_{chill,in} - T_{chill,out}) \end{aligned} \quad (6)$$

$$\begin{aligned}
& (m_{\text{con}} C_{p,\text{con}} + m_{\text{con,hex}} C_{p,\text{hex}}) \frac{dT_{\text{con,ref}}}{d\tau} \\
& = -h_{fg} m_a \frac{dx_{\text{des}}}{d\tau} + m_a C_{p,v,\text{ref}} (T_{\text{con}} - T_{\text{bed}}) \\
& \quad + \dot{m}_{f,\text{con}} C_{p,f} (T_{\text{con,in}} - T_{\text{con,out}}) \quad (7)
\end{aligned}$$

Similar approach as Eq. (4) can be applied in Eqs. (6) and (7), and the LMTD equations used for evaporator and condenser are as shown below

$$\frac{T_{\text{chill,out}} - T_{\text{eva}}}{T_{\text{chill,in}} - T_{\text{eva}}} = \exp \left[-\frac{(UA)_{\text{eva,ref}}}{\dot{m}_{f,\text{chill}} C_{p,f}} \right] \quad (8)$$

$$\frac{T_{\text{con,out}} - T_{\text{con}}}{T_{\text{con,in}} - T_{\text{con}}} = \exp \left[-\frac{(UA)_{\text{con,ref}}}{\dot{m}_{f,\text{con}} C_f} \right] \quad (9)$$

The cooling capacity can be obtained from the evaporator and can be calculated by the following equation:

$$Q_{\text{eva,cycle}} = \frac{1}{\tau_{\text{cycle}}} \int_0^{\tau_{\text{cycle}}} (\dot{m} C_p)_w (T_{\text{chill,in}} - T_{\text{chill,out}}) d\tau \quad (10)$$

The driving source temperature can be expressed as Eq. (11). Finally, the COP of the adsorption chiller can be obtained from Eq. (12), as follows:

$$Q_{\text{hot,ref}} = \frac{1}{\tau_{\text{cycle}}} \int_0^{\tau_{\text{cycle}}} (\dot{m} C_p)_{\text{des}} (T_{\text{hot,in}} - T_{\text{hot,out}}) d\tau \quad (11)$$

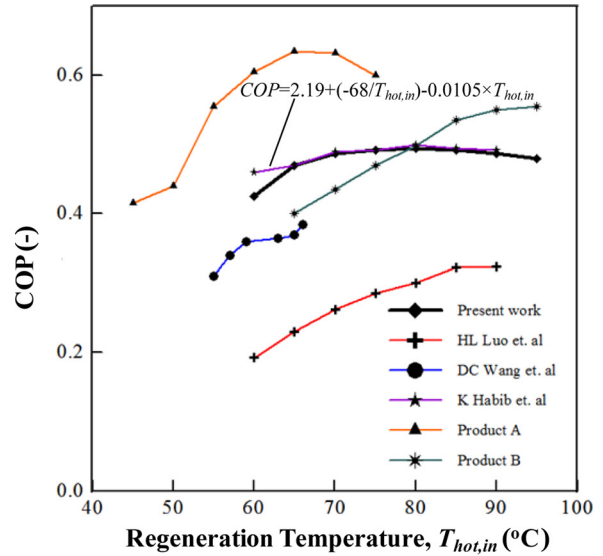
$$\text{COP} = \frac{Q_{\text{hot,ref}}}{Q_{\text{eva,cycle}}} \quad (12)$$

Since an adsorption chiller is commonly used for cooling purpose only when the ambient temperature is hot, the heat sink is usually almost constant. Thus, its performance can be simply estimated by only using the regeneration temperature. The relation between regeneration temperature with cooling capacity and COP is shown in Figs. 3(a) and 3(b), respectively. Since maximum cooling capacity ($Q_{\text{cap,max}}$) is different from one adsorption chiller to another adsorption chiller, it should be noted that the cooling capacity shown in Fig. 3(a) is the dimensionless values of ratio between the cooling capacity to the maximum cooling capacity. Cooling capacity and COP of the model were compared to other silica gel–water adsorption chillers. Performance of other adsorption chillers was reported by Zhai and Wang [18], Luo et al. [19], Wang et al. [20], Product A [21], and Product B [22]. It was found that the performance of the adsorption chiller model is comparable with other adsorption chillers. The adsorption chiller presented by Luo had lower COP most probably because the design optimization on the system components including heat exchangers and adsorption bed was not thoroughly carried out.

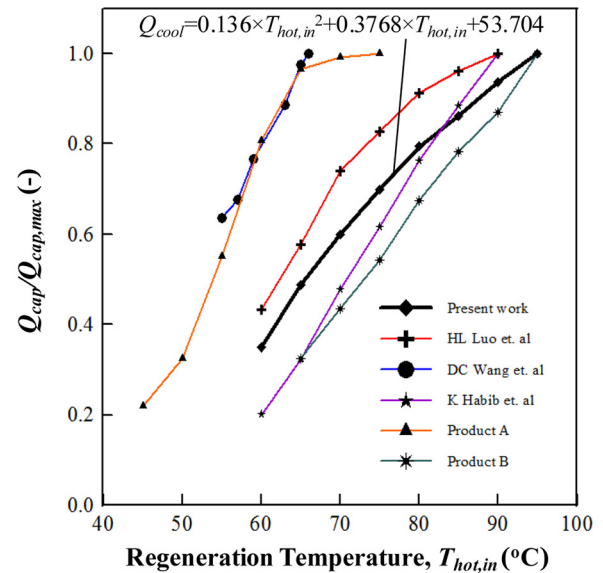
It should be noted that this model supplied cooling energy based on the temperature and amount of hot water delivered to the adsorption chiller. Thus, solar water heater needs to supply sufficient amount and sufficient temperature of hot water to the adsorption chiller.

2.4 Solar Water Heater. The schematic diagram of the overall system is shown in Fig. 4. Solar energy is collected by the flat-plate collectors and supplied to the adsorption chiller through heat exchangers and a hot water tank. If heat from the solar water heater is insufficient to achieve the desired cooling, the auxiliary heater will be operated. It should be noted that the efficiency of heat exchangers and auxiliary heater was assumed to be constant at 0.80.

Solar AC with five different values of SF: 0.33, 0.50, 0.74, 0.89, and 0.98 was studied as shown in Table 3. Other parameters



(a)



(b)

Fig. 3 Relation between regeneration temperature with cooling capacity and COP: (a) cooling capacity and regeneration temperature and (b) COP and regeneration temperature

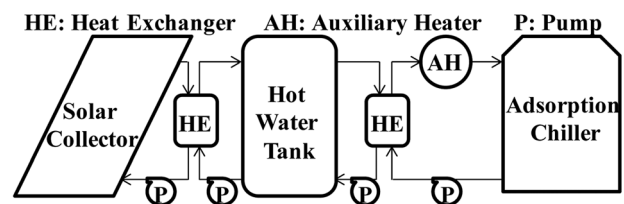


Fig. 4 Schematic diagram of the solar water heater

including the panel area, pump flow rate, pipe length, and hot water tank volume that vary depending on the SF are also shown. The selection of ratio between thermal storage size to the solar panel area of 50 L/m² was carried out. This value was sufficient to deliver the desired amount and temperature of the hot water outlet. This value may slightly varies because of the setting of initial

Table 3 Parameters for different SF

SF (—)	Panel area (no. of panel) m ² (unit)	Pump flow rate (kg/s)	Pipe length (m)	Tank volume (m ³)
0.33	19.9 (10)	0.44	52	1.0
0.50	29.9 (15)	0.66	66	1.5
0.74	39.8 (20)	0.88	80	2.0
0.89	49.8 (25)	1.10	94	2.5
0.98	59.7 (30)	1.32	108	3.0

Table 4 Basic parameters of the flat-plate collector

Type	Glazed flat-plate	
Dimension	m	2.016 × 0.985 × 0.077
Gross area	m ²	1.99
Dry weight	kg	34
Nominal flow rate	kg/s	0.044
Tilt angle	deg	10

Table 5 Parameters used for the life-cycle cost analysis

		1 US\$ = RM3
Exchange rate		1 US\$ = RM3
Electricity tariff	US\$/kWh	First 200 kWh, 0.145 After 200 kWh, 0.170
Gas tariff	US\$/m ³	0.197
Lifetime	yr	25
Interest rate	—	0.035
Initial cost		
Adsorption chiller	US\$/kW	800
Flat-plate collector	US\$/m ²	300
Heat storage	US\$/m ³	5500
Electric heater	US\$/kW	125
Gas boiler	US\$/kW	90
Water pump	US\$/(m ³ /hr)	100
Pipeline	US\$/m	50

temperature, tank basement temperature, thermal storage medium, and heat loss coefficient of the thermal storage.

2.5 Flat-Plate Collectors. For the solar heat collector, test data of a commercial flat-plate were used as the model of the collector. Table 4 shows the basic parameters of the flat-plate collector. It was a glazed collector with an area of 1.99 m² each with mass flow rate of 0.044 kg/s.

2.6 SF and Life-Cycle Cost Analysis. Heat from solar and auxiliary heater is supplied to the adsorption chiller for AC purpose. The SF is defined as the ratio of annual average solar energy to the annual average total energy delivered to the adsorption chiller and can be calculated by the following equation:

$$SF = \frac{Q_{SWH,ave}}{Q_{del,ave}} = \frac{Q_{del,ave} - Q_{AH,ave}}{Q_{del,ave}} \quad (13)$$

where $Q_{SWH,ave}$ is the annual average heat from solar water heater (kW), $Q_{del,ave}$ is the annual average heat load delivered (kW), and $Q_{AH,ave}$ is the annual average heat from auxiliary heater (kW).

Life-cycle cost analysis which considers time value of money was used to evaluate the economic performance of the AC system. All cashflow throughout the life cycle were calculated based on present worth value. The NP gained for 25 yr of life cycle of the investment on the energy system can be calculated by the following equation:

Table 6 Capacity and unit for different values of SF

		0.33	0.50	0.74	0.89	0.98
Adsorption chiller	kW	16	16	16	16	16
Solar collector	m ²	19.9	29.9	39.8	49.8	59.7
Heat storage	m ³	1.0	1.5	2.0	2.5	3.0
Auxiliary heater	kW	19.2	16.5	13.1	13.1	13.1
Water pump	m ³ /hr	1.5	2.4	3.2	4.0	4.8
Pipeline	m	52	66	80	94	108

Table 7 Emissions rate for typical CST, CCGT, and natural gas boiler

CO ₂	CST	g/kWh _p	965
	CCGT	g/kWh _p	363
	Boiler	g/kWh _{th}	201
NO _x	CST	g/kWh _p	1.7
	CCGT	g/kWh _p	0.20
	Boiler	g/kWh _{th}	0.22
CO	CST	g/kWh _p	0.07
	CCGT	g/kWh _p	0.07
	Boiler	g/kWh _{th}	0.12

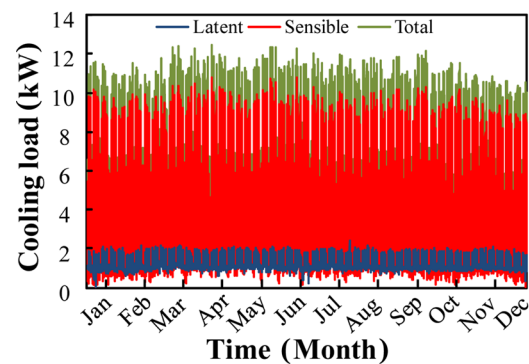


Fig. 5 Cooling load of the building throughout the year

$$NP = Rev_{elec.sav.} - (C_{eq} + C_{ins} + C_{AH-ener.}) \quad (14)$$

where $Rev_{elec.sav.}$ is the revenue from electricity saving (US\$), C_{eq} is the equipment cost (US\$), C_{ins} is the installation cost (US\$), and $C_{AH-ener.}$ is the cost of energy for the auxiliary heater (US\$). The cost of installation was also considered and assumed to be 10% of the total cost. The energy for the auxiliary heater can be electricity or natural gas.

Revenue from electricity saving and operational cost of energy for auxiliary heater is a series of cashflow in the future. Present worth factor (PWF) needs to be calculated to obtain their present value. The PWF can be calculated by the following equation:

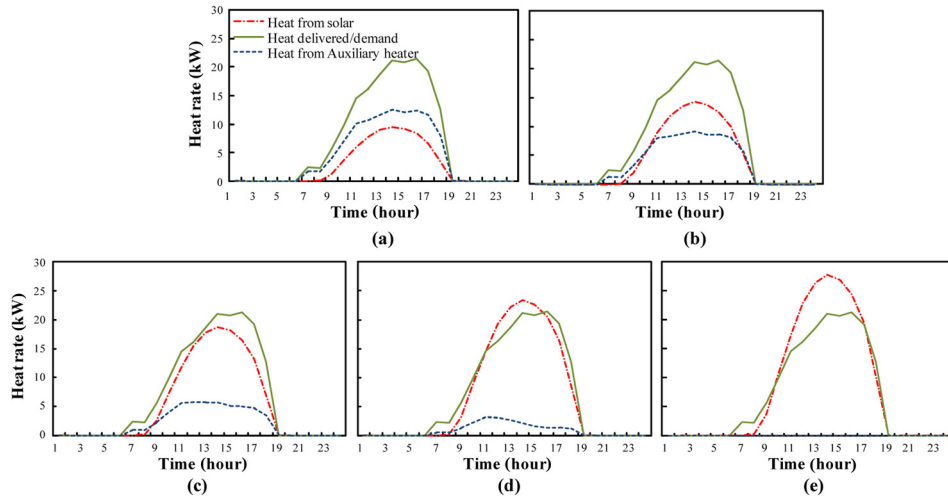


Fig. 6 Heat balance throughout a day for different SF values: (a) SF = 0.33, (b) SF = 0.50, (c) SF = 0.74, (d) SF = 0.89, and (e) SF = 0.98

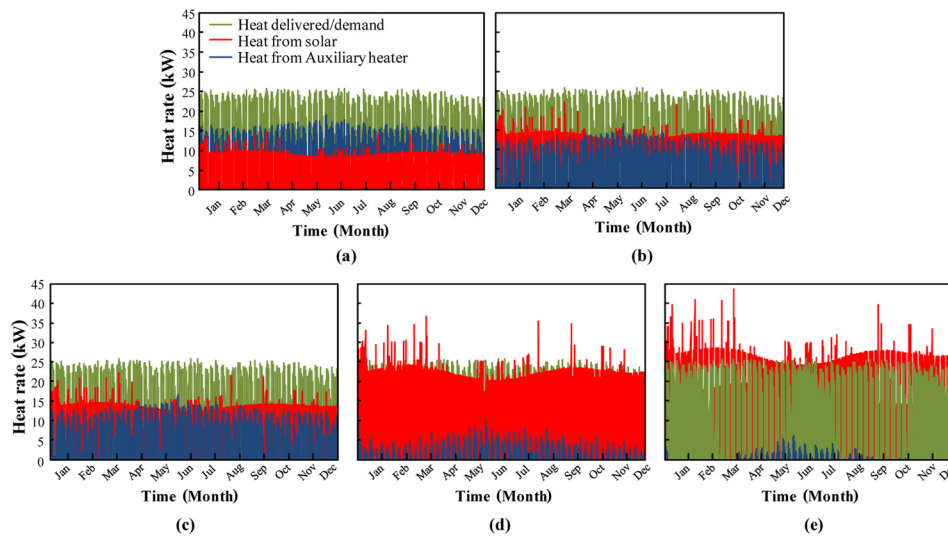


Fig. 7 Heat balance throughout a year for different SF values: (a) SF = 0.33, (b) SF = 0.50, (c) SF = 0.74, (d) SF = 0.89, and (e) SF = 0.98

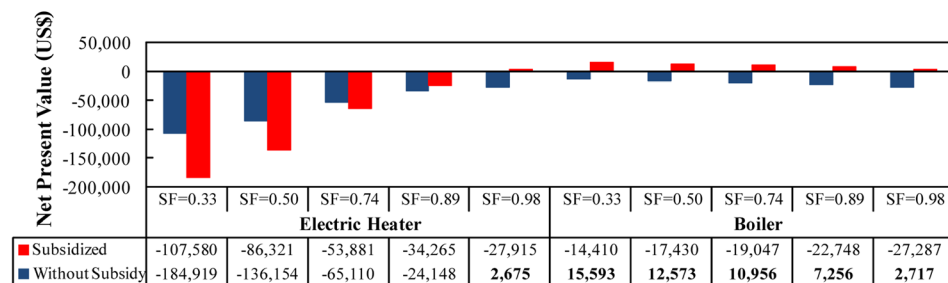


Fig. 8 Result of life-cycle cost analysis

$$PWF_x = \frac{(1+i)^n - 1}{i(1+i)^n} \quad (15)$$

where i and n are the lifetime (year) and interest/discount rate (-), respectively. Interest rate, lifetime, and other parameters used for the life-cycle cost calculation are shown in Table 5 [9,23].

Moreover, capacity and unit for every SF for all equipment are shown in Table 6.

2.7 Emissions From Different Solar AC Systems. Both solar AC and conventional AC release emissions, either on site or from the power plant that supplies electricity. If electricity-powered auxiliary heater or conventional AC is used, typical

emissions rate from a power plant was considered, whereas when natural gas-fired auxiliary heater is used, typical emissions rate from a natural gas boiler was considered. Two types of power plants were considered: the common coal steam turbine (CST) and the high-end combined cycle gas turbine (CCGT) plant. Emissions rate of these energy systems is shown in Table 7 [24].

3 Results and Discussion

3.1 Cooling Load of the Building and Heat Balance of the System. Figure 5 shows sensible and latent cooling load of the building throughout the year. Latent cooling load was mainly from building infiltration and occupant in the building. Figure 5 shows that the latent cooling load was much lower which is in the range of 0–2.3 kW, whereas the sensible cooling load was in the range of 0–10.8 kW. However, this indicates that if a solar desiccant system is integrated to the AC system, the latent cooling load can be drastically reduced and solar AC with a better performance can be achieved.

Figure 6 shows the heat balance between heat demand/delivered, heat from solar and auxiliary energy for a randomly selected day, 1st February. Result for SF from 0.33 to 0.98 is shown in Figs. 6(a)–6(e). As shown in the figure, as the SF increased, the portion of heat from solar increased, whereas the auxiliary energy decreased. However, the heat balance was not totally matched especially for SF of 0.98, where heat from solar was higher than heat demand. This is because of the existence of preheat tank where heat is stored, and also the targeted temperature in which the quality of the heat is also considered. Thus, heat from solar is sometimes higher and sometimes lower than the heat demand/delivered.

The result of heat balance throughout the year is shown in Fig. 7. It has similar trend with the result for a single day, with auxiliary energy decreased when SF increased. It further shows there was slight fluctuation of auxiliary energy, due to variation of solar radiation throughout the year. Even the highest value of SF (SF = 0.98) still needs auxiliary energy from March to September during which period the solar radiation was comparatively lower.

3.2 Life-Cycle Cost of the System. The NP throughout the life-cycle cost analysis is shown in Fig. 8. The right side of the figure represents the case when a natural gas-fired boiler was used as the auxiliary heater, whereas left side of figure represents the case when an electric heater was used. Since electricity is heavily subsidized in Malaysia, unsubsidized electricity priced which is roughly assumed at two times higher was also considered for each SF.

As shown in Fig. 8, none of the SF can generate NP under subsidized electricity price. High capital cost of the adsorption chiller and solar collector is the main factor that makes installation of solar AC still unattractive at the moment. The government needs to provide incentive or subsidy for installation of the solar cooling system. This result is inline with what was reported in Refs. [12–14]. When unsubsidized electricity price was considered, all SF values for a natural gas boiler and an electric heater only with SF of 0.98 can generate the NP. This shows that a boiler is a better auxiliary heater than electric heater because the gas price is cheaper than electricity.

When an electric heater was used, higher NP can be obtained at higher SF because of the reduction of operational cost (electricity for backup heater). Solar AC with electric heater as backup can only generate NP under unsubsidized electricity price at the SF of 0.98.

When a boiler was used, higher NP was found at lower values of SF. This is because of the difference of fuel cost reduced and initial cost required between SF values of 0.30 and 0.98. When the SF increased, the NP decreased because the initial cost was higher than fuel cost saved. The highest NP was US\$15,593 at SF value of 0.33.

It should be noted that the results of this analysis were based on the cooling load of an office building that operated 08:00–17:00,

Monday to Friday throughout the year. If the solar AC is used for other buildings with lower buildings usage, revenue will decrease and therefore the NP will be less.

3.3 Emissions Performance. Comparison of emissions released between solar AC, with different SF, and conventional systems is shown in Fig. 9. CO₂, NO_x, and CO emissions are

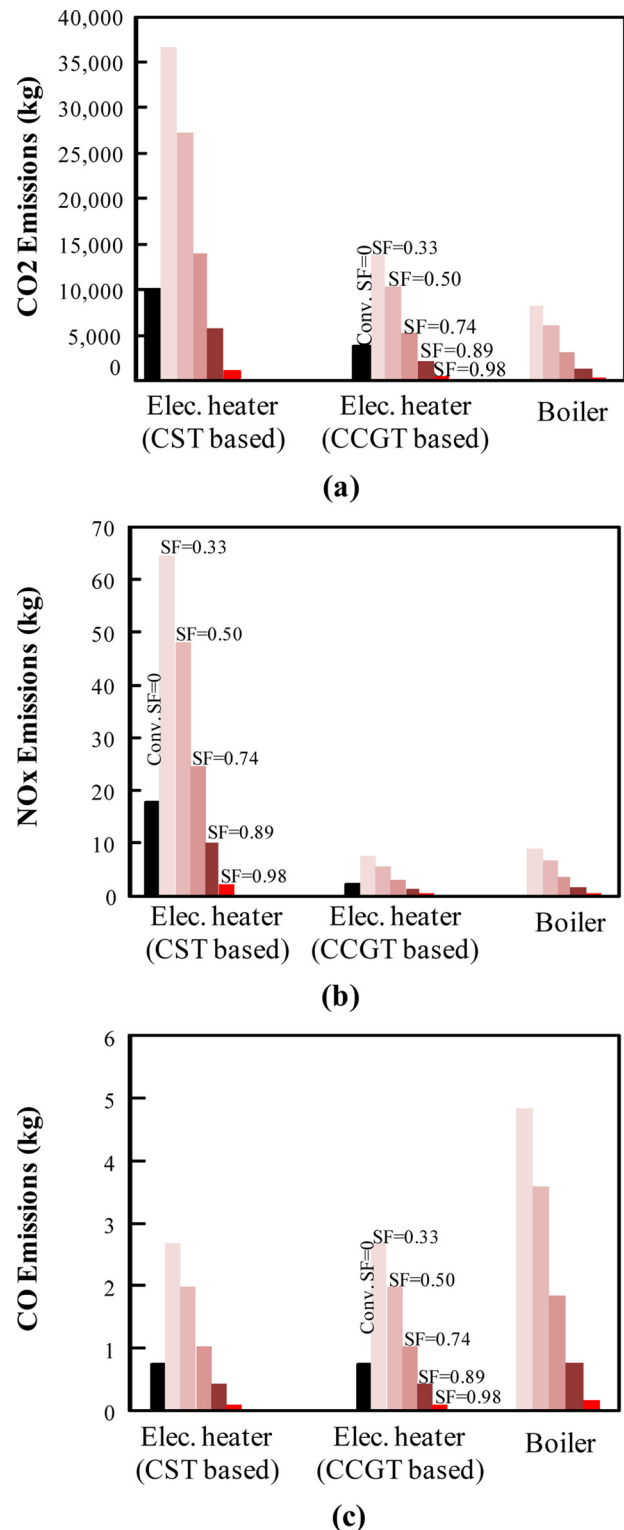


Fig. 9 Comparison of emissions released from solar AC with different SF values, and conventional systems: (a) CO₂ emissions, (b) NO_x emissions, and (c) CO emissions

shown in Figs. 9(a)–9(c), respectively. The electricity supplied considered were CST and CCGT. In each figure, cases of electric heater (CST based), electric heater (CCGT based), and boiler are shown. Conventional system that represents vapor compression AC was also shown as the reference case. It was found that in overall, electric heater (CST based) had the highest CO₂ and NO_x emissions, and electric heater (CCGT based) and boiler had the similar level of emissions, except for CO. This again shows that boiler is a better solution for auxiliary heater, not only in terms of economic as shown in Sec. 2 but also in terms of environmental performance.

It was also found that when the SF increased, all types of emissions decreased for all cases of backup heater. However, all emissions types released from the solar AC were higher than the vapor compression AC, especially when the SF is lower than 74% for all cases. Although the amount of emissions for this single building is small, considering the rapid growth of AC usage as stated in Sec. 1, the environmental impact from the usage of AC could not be neglected.

Although the life-cycle cost analysis in Sec. 3.2 clarified that using a boiler at lower SF is the best option in terms of economic performance, lower SF in this section shows that solar AC releases more emissions as compared to a conventional AC. This could cancel out the benefit of the solar AC, which is a sustainable AC system. Thus, the most appropriate SF for a solar AC is around 0.74 when economic and environmental performance are fairly considered.

4 Conclusions

A solar AC system that needs to cover cooling demand for an office building in Kuala Lumpur was studied. There was no conventional AC used as a backup AC, but cooling demand is fully covered by a solar AC with an auxiliary heater used as backup heat source. Results show that none of the SF can generate NP under subsidized electricity price. Thus, solar AC is not attractive because of the high capital cost of the adsorption chiller and solar heat collector. When unsubsidized electricity price was considered, all values of the SF for a natural gas boiler and an electric heater with only SF of 0.98 can generate NP. Life-cycle cost and emissions analysis show that a natural gas boiler is a better auxiliary heater than an electric heater because the gas price is cheaper and it has lower emissions. Furthermore, it was also found that lower SF can generate higher NP. The highest NP was US\$15,600 at SF value of 0.33 when a boiler was used. However, the environmental performance shows that lower SF value releases more emissions as compared to a conventional AC. This cancels out the benefit of the solar AC, which is a sustainable AC system. Since most of the cases of solar AC with SF of 0.74 above can reduce emissions compared to a conventional AC, when environmental and economic performance are fairly considered, the most appropriate SF for a solar AC is around 0.74.

Acknowledgment

The authors gratefully acknowledge Universiti Malaysia Pahang and Ministry of Education Malaysia for funding this research under FRGS/1/2014/TK06/UMP/2001/1 or RDU140119.

Nomenclature

Symbols

A = area, m²
 C = cost, US\$
 C_p = specific heat, J/kg K
COP = coefficient of performance
 D_{so} = pre-exponential constant, m²/s
 E_a = activation energy, J/kg
 G_{glob} = global radiation, W/m²
 h = enthalpy, J/kg

h_{fg} = latent heat of vaporization, J/kg
 i = interest/discount rate
 m = mass, kg
 \dot{m} = mass flow rate, kg/s
NP = net profit, US\$
 P_s = saturation pressure, Pa
PWF = present worth factor
 Q = heat rate, kW
 R_p = fiber radius of silica gel, m
Rev = revenue, US\$
 T = temperature, °C or K
 U = overall heat transfer coefficient, W/m² K
 x = adsorption uptake, kg/kg
 x = instantaneous uptake, kg/kg
 x^* = equilibrium uptake, kg/kg
 α_0 = coefficient in Eq. (3) (kg (kg of dry adsorbent)⁻¹)
 α_1 = coefficient in Eq. (3) (kg (kg of dry adsorbent, K)⁻¹)
 α_2 = coefficient in Eq. (3) (kg (kg of dry adsorbent, K²)⁻¹)
 α_3 = coefficient in Eq. (3) (kg (kg of dry adsorbent, K³)⁻¹)
 β_0 = coefficient in Eq. (3)
 β_1 = coefficient in Eq. (3), K⁻¹
 β_2 = coefficient in Eq. (3), K⁻²
 β_3 = coefficient in Eq. (3), K⁻³
 Δh_{st} = isosteric heat of adsorption, J/kg
 τ = time, s

Subscripts

a = adsorbent
amb = ambient
AH = auxiliary heater
AH-ener = auxiliary heater energy consumption
bed = adsorber or desorber bed
bed = sorption heat exchanger (adsorber or desorber)
chill = chilled water
con = condenser
cycle = cycle time
del = delivered
elec.sav = electricity saved
eq = equipment
eva = evaporator
 f = liquid phase refrigerant
hex = heat exchanger
in = inlet
ins = installation
out = outlet
ref = refrigerant
SWH = solar water heater
 v = vapor phase refrigerant

Abbreviation

CCGT = combined cycle gas turbine
CST = coal steam turbine

References

- [1] Mahlia, T. M. I., Masjuki, H. H., and Choudhury, I. A., 2002, "Potential Electricity Savings by Implementing Energy Labels for Room Air Conditioner in Malaysia," *Energy Convers. Manage.*, **43**(16), pp. 2225–2233.
- [2] Mahlia, T. M. I., Masjuki, H. H., Choudhury, I. A., and Saidur, R., 2001, "Potential CO₂ Reduction by Implementing Energy Efficiency Standard for Room Air Conditioner in Malaysia," *Energy Convers. Manage.*, **42**(14), pp. 1673–1685.
- [3] Qian, S., Gluesenkamp, K., Hwang, Y., Rademacher, R., and Chun, H., 2013, "Cyclic Steady State Performance of Adsorption Chiller With Low Regeneration Temperature Zeolite," *Energy*, **60**, pp. 517–526.
- [4] Rezk, A. R. M., and Al-Dadah, R. K., 2012, "Physical and Operating Conditions Effects on Silica Gel/Water Adsorption Chiller Performance," *Appl. Energy*, **89**(1), pp. 921–929.
- [5] Aristov, Y. I., Glaznev, I. S., and Gimik, I. S., 2012, "Optimization of Adsorption Dynamics in Adsorptive Chillers: Loose Grains Configuration," *Energy*, **46**(1), pp. 484–492.

- [6] Niazmand, H., Talebian, H., and Mahdavihah, M., 2012, "Bed Geometrical Specifications Effects on the Performance of Silica/Water Adsorption Chillers," *Int. J. Refrig.*, **35**(8), pp. 2261–2274.
- [7] Lu, Z. S., Wang, R. Z., Xia, Z. Z., Lu, X. R., Yang, C. B., Ma, Y. C., and Ma, G. B., 2013, "Study of a Novel Solar Adsorption Cooling System and a Solar Absorption Cooling System With New CPC Collectors," *Renewable Energy*, **50**, pp. 299–306.
- [8] Spencer, J. D., Moton, J. M., Gibbons, W. T., Gluesenkamp, K., Ahmed, I. I., Tavemer, A. M., McGahagan, D., Tesfaye, M., Gupta, C., Boume, R. P., Monje, V., and Jackson, G. S., 2013, "Design of a Combined Heat, Hydrogen, and Power Plant From University Campus Waste Streams," *Int. J. Hydrogen Energy*, **39**(12), pp. 4889–4900.
- [9] Bruno, J. C., Lopez-Villada, J., Ortega, J., and Coronas, A., 2006, "Techno-Economic Design Study of a Large-Scale Solar Cooling Plant Integrated in a District Heating and Cooling Network," 61st ATI National Congress, Solar Heating and Cooling International Session, Perugia, Italy, Sept. 12–15, pp. 227–232.
- [10] Balaras, C. A., Grossman, G., Henning, H.-M., Ferreira, C. A. I., Podesser, E., Wang, L., and Wiemken, E., 2007, "Solar Air Conditioning in Europe—An Overview," *Renewable Sustainable Energy Rev.*, **11**(2), pp. 299–314.
- [11] Ferreira, C. I., and Kim, D.-S., 2014, "Techno-Economic Review of Solar Cooling Technologies Based on Location-Specific Data," *Int. J. Refrig.*, **39**, pp. 23–37.
- [12] Tsoutsos, T., Anagnostou, J., Pritchard, C., Karagiorgas, M., and Agoris, D., 2003, "Solar Cooling Technologies in Greece. An Economic Viability Analysis," *Appl. Therm. Eng.*, **23**(11), pp. 1427–1439.
- [13] Lambert, M. A., and Beyene, A., 2007, "Thermo-Economic Analysis of Solar Adsorption Heat Pump," *Appl. Therm. Eng.*, **27**(8–9), pp. 1593–1611.
- [14] Fasfous, A., Asfar, J., Al-Salaymeh, A., Sakhrieh, A., Al_hamamre, Z., Al-bawwab, A., and Hamdan, M., 2013, "Potential of Utilizing Solar Cooling in the University of Jordan," *Energy Convers. Manage.*, **65**, pp. 729–735.
- [15] Allouhi, A., Kouksou, T., Jamil, A., El Rhafiki, T., Mourad, Y., and Zeraoui, Y., 2015, "Economic and Environmental Assessment of Solar Air-Conditioning Systems in Morocco," *Renewable Sustainable Energy Rev.*, **50**, pp. 770–781.
- [16] Mammoli, A., Vorobieff, P., Barsun, H., Burnett, R., and Fisher, D., 2010, "Energetic, Economic and Environmental Performance of a Solar-Thermal-Assisted HVAC System," *Energy Build.*, **42**(9), pp. 1524–1535.
- [17] Hang, Y., Qu, M., and Zhao, F., 2011, "Economic and Environmental Assessment of an Optimized Solar Cooling System for a Medium-Sized Benchmark Office Building in Los Angeles, California," *Renewable Energy*, **36**(2), pp. 648–658.
- [18] Zhai, X. Q., and Wang, R. Z., 2009, "Experimental Investigation and Theoretical Analysis of the Solar Adsorption Cooling System in a Green Building," *Appl. Therm. Eng.*, **29**(1), pp. 17–27.
- [19] Luo, H. L., Dai, Y. J., Wang, R. Z., Wu, J. Y., Xu, Y. X., and Shen, J. M., 2006, "Experimental Investigation of a Solar Adsorption Chiller Used for Grain Depot Cooling," *Appl. Therm. Eng.*, **26**(11–12), pp. 1218–1225.
- [20] Wang, D. C., Shi, Z. X., Yang, Q. R., Tian, X. L., Zhang, J. C., and Wu, J. Y., 2007, "Experimental Research on Novel Adsorption Chiller Driven by Low Grade Heat Source," *Energy Convers. Manage.*, **48**(8), pp. 2375–2381.
- [21] InvenSor, 2013, "InvenSor LTC 10 Plus," InvenSor GmbH, Lutherstadt Wittenberg, Germany.
- [22] InvenSor, 2013, "InvenSor HTC 18 Plus," InvenSor GmbH, Lutherstadt Wittenberg, Germany.
- [23] Basrawi, F., Yamada, T., and Obara, S., 2014, "Economic and Environmental Based Operation Strategies of a Hybrid Photovoltaic–Microgas Turbine Trigenation System," *Appl. Energy*, **121**, pp. 174–183.
- [24] Strachan, N., and Farrell, A., 2006, "Emissions From Distributed Versus Centralized Generation: The Importance of System Performance," *Energy Policy*, **34**(17), pp. 2677–2689.